PNAS
www.pnas.org

Supplementary Information for
Protective role of chaperone-mediated autophagy against atherosclerosis

Julio Madrigal-Matute[a,b], Jenny de Bruijn[c], Kim van Kuijk[c], Dario F Riascos-Bernal[d], Antonio Diaz[a,b], Inmaculada Tasset[a,b], Adrián Martín-Segura[a,b], Marion J.J. Gijbel[c,e], Bianca Sander[c], Susmita Kaushik[a,b], Erik A.L. Biessen[c], Simoni Tiano[a,b], Mathieu Bourdenx[a,b], Gregory J. Krause[a,b], Ian McCracken[f], Andrew Baker[f], Han Jin[c], Nicholas Sibinga[a,d], Jose Javier Bravo-Cordero[g], Fernando Macian[h], Rajat Singh[a,b,d], Patrick C.N. Rensen[j], Jimmy F.P. Berbée[j†], Gerard Pasterkamp[k], Judith C. Sluimer[c,f,1], Ana Maria Cuervo[a,b,d,1].

[1]To whom correspondence may be addressed: Ana Maria Cuervo MD PhD, ana-maria.cuervo@einsteinmed.edu and Judith Sluimer PhD, judith.sluimer@maastrichtuniversity.nl

This PDF file includes:

Supplementary text
Figures S1 to S7
Tables S1 to S6
SI References

Other supplementary materials for this manuscript include the following:

Dataset S1

Supplementary Information Text

Extended Methods

Animal models and treatments

KFERQ-PS-Dendra2 mice (1) were generated by donor egg injection in wild type FVB mice using the pRP.ExSi plasmid backbone with the insert coding for 11 amino acids including the KFERQ sequence of RNase A in frame with the sequence of Dendra2 under the hybrid promoter CAGG and crossed back more than 9 generations to C57BL/6J. Male C57BL/6J LAMP-2A knock-out (L2AKO) were generated as described before (2). C57BL/6J mice conditionally expressing hLAMP-2A (hL2AOE) (3) were generated by inserting the hLAMP-2A cDNA sequence with a STOP cassette (a neo cassette flanked by two Loxp sites) into mouse ROSA26 locus in PTL1 (129B6 hybrid) ES cells that were used to generate heterozygous mice carrying the ROSA26-STOP-hLAMP-2A allele. Crossing these mice with ^{Tmx}ER-Cre mice generated a mouse line in which expression of hLAMP-2A could be induced by injection of tamoxifen (TMX) (4 intraperitoneal (i.p.) injections of 20 mg/kg b.w. on alternate days). Male mice (KFERQ-PS-Dendra2, WT, L2AKO, CTRL and hL2AOE) were intraorbitally injected at 12 weeks of age with a single dose of AAV8-PCSK9 ($1.0x10^{11}$VC) to promote the degradation of LDLR and increase circulating cholesterol levels (4). Atherosclerosis was further induced by feeding the mice a Western-type diet (WD; D12108; ResearchDiets; saturated fats (35 kcal%), cholesterol (1.25% w/w) and cholic acid (0.22% w/w)) for 12 weeks. KFERQ-PS-Dendra2, WT and L2AKO mice were fed a WD for 12 weeks and sacrificed for further analysis. After 6 weeks on diet, when we observed the drop in CMA activity, CTRL and hL2AOE were injected with TMX to activate expression of hLAMP-2A and all mice were monitored for 10 additional weeks (3). This longer protocol was required to compensate for the reduced intestinal absorption of cholesterol observed in the first 2 weeks upon TMX injection (5). Mice were all in the C57BL/6J background and housed in ventilated cages with no more than 5 mice per cage on a 12h light/dark cycle at 23°C with free access to water and food in the institutional barrier facility along with sentinel cages and were specific pathogen-free. Genotyping, breeding and treatments in this study were done accordingly to protocol and all animal studies were under an animal study protocol approved by the Institutional Animal Care and Use Committee of Albert Einstein College of Medicine.

Primary cell cultures, cell lines and treatments

VSMC were isolated from 8 weeks old mice aortas (pool of 5 mice per genotype) by collagenase digestion and maintained in DMEM (Gibco) supplemented with 20% fetal bovine serum (FBS, Gibco), 2mM L-glutamine, 100 U/ml penicillin and 100 µg/ml streptomycin (Invitrogen). LPDS was prepared from FBS delipidated with 4% fumed silica (6). VSMC were incubated for 24h in DMEM media plus 5% LPDS with or without LDL (150 μg/ml LDL-cholesterol) plus 0.1 U/ml of bovine lipoprotein lipase (7). For DiI-LDL production, LDL was labeled with the fluorescent probe DiI (Invitrogen) as previously described (8).

Bone marrow derived macrophages (BMDM) were isolated from 8 weeks old mice and differentiated in non-treated tissue culture plates by using Iscove's Modified Dulbecco's medium (IMDM) containing 20% of FBS and supplemented with 20% of L-929 cells conditioned media. After 5 days in culture, nonadherent cells were eliminated and adherent cells were trypsinized and seeded into the final plates for treatment (6). Macrophage stimulation was attained by removing the culture medium and culturing cells for an additional 18h in DMEM supplemented with 5% FBS (for CTRL) or 5% FBS, 20 ng/ml IFN-γ, and 100 ng/ml LPS (for IFN-γ/LPS) (9).

Human samples

Tissue samples and human mRNA and RNAseq data included in this study are from 4 different cohorts as follows (see also **Tables S2** and **S3**).

Study 1: Human carotid plaque samples (n=37, mean age 72 years, 64% men) representing the following stages of atherosclerosis: intimal thickening, pathological intimal thickening, thick fibrous cap (stable) atheroma, and plaque with intraplaque hemorrhage, were obtained anonymously at autopsy from subjects without cardiovascular symptoms and no additional clinical information was collected. Collection, storage and use of tissues were performed in agreement with the Dutch Code for Proper Secondary use of Human Tissue. An opt-out

arrangement was in place at time of hospital admission, and hence tissues were not used in case of objection by relatives in line with the guidelines provided by the Dutch Code for Proper Secondary use of Human Tissue. None of the co-authors were directly involved with tissue collection.

Study 2: mRNA expression by microarray analysis was obtained from previously published studies (10). Briefly, atherosclerotic plaque samples were obtained during carotid endarterectomy (n=36 symptomatic patients, mean age 72.9 years, age range 64-83 years, 100% men, clinical characteristics in Supplementary Table 1 of (10)). All experiments were conducted in agreement with the code for proper secondary use of human tissue in the Netherlands (http://www.fmwv.nl). Plaques were segmented for histology, and flanked segments used for RNA isolation. Classification of all used plaques was performed on H&E-stained slides according to Virmani *et al (11)*, by experienced cardiovascular pathologists (JCS, MG). Plaques with and without intraplaque hemorrhage were compared. No follow-up is available.

Study 3: Single cell RNAseq data was obtained from previously published studies (12). Briefly, human coronary arteries dissected from explanted hearts of transplant recipients were obtained from the Human Biorepository Tissue Research Bank under the Department of Cardiothoracic Surgery from consenting patients, with approval from the Stanford University Institutional Review Board (n=4, ages 65, 54, 65 and 58 years, 100% men, clinical characteristics in Supplementary Table 4 of (12)). Histology is not available.

Study 4: Human atherosclerotic plaques were from the AtheroExpress Study biobank (13), in which plaques from patients undergoing carotid endarterectomy were obtained and segmented for serial histology or snap frozen for protein/RNA isolation. Patients were included if they suffered a symptomatic ischemic event within 6 months prior to the surgery. Plaques were segmented for histology and adjacent protein isolation. After surgery, patients were followed up for a minimum of three years to assess if they underwent a secondary major adverse cardiovascular event or not. Subjects with one event at baseline were compared with subjects who also had a second event at follow-up (n= 62, mean age 68.8, age range 63-74 years, 64.2% men, clinical characteristics per group shown in **Table S3**). This study complies with the Declaration of Helsinki, and the local Medical Ethical Committee in accordance with national regulations approved use of this tissue (protocol number 16-4-181 and O3-114O).

In the analysis of aortas from individuals of different ages RNAseq data was obtained from the GTEx portal (14) (https://gtexportal.org (dbGaP Study Accession: phs000424.v8.p2) and single cell RNAseq data was from the Tabula Sapiens (15) (https://tabula-sapiens-portal.ds.czbiohub.org/). Details of these studies are summarized in **Table S2**).

Antibodies

Primary antibodies were from the following sources (dilutions, commercial source and catalog number indicated in brackets): rat anti-LAMP2 (1/500, Hybridoma Bank, GL2A7), rabbit anti-LAMP-2A (1/5000, Thermo Scientific, 512200), rabbit anti-LDLr (1/1000, Abcam, ab52818), rabbit anti-human LAMP-2A (1/1000, Abcam, ab18528), rat anti-LAMP1 (1/500, Hybridoma Bank, 1D4B), mouse anti-human LAMP2 (1/500, Hybridoma Bank, H4B4), rabbit anti-LC3 (1/1000, Cell Signaling, 2775), rabbit anti-P62 (Enzo Life Sciences BMLPW98600100), anti-CD68 (rat, 1/200 Bio-Rad, mca1957; rabbit, ab125212, Abcam), anti-α-SMA (rabbit, 1/500 Abcam, ab202510; mouse, F3777, Sigma; mouse, M0851, Dako), goat anti-Cathepsin D (1/500, Santa Cruz, sc-6486), mouse IgM anti-HSC70 (1/5000, Novus Biologicals, nb120-2788), rabbit anti-iNOS (1/1000, Cell Signaling 2977), rabbit anti-COX-2 (1/1000, Cell Signaling, 12282), mouse anti-p53 (1/1000, Cell Signaling, 2524), rabbit anti-P27 (1/1000, Cell Signaling, 2552), rabbit, anti-P21 (1/1000, Abcam, ab109199) and anti-HMGB1 (1/1000, Abcam, ab18256). All the secondary antibodies were from Thermo Scientific. All antibodies used in this study were from commercial sources and were validated following the multiple dilution method and, where available, using cell lines or tissues from animals knock-out for the antigen. Sources of chemicals were as described before (2, 16).

Tissue dissection and Histological Procedures

All mice were euthanized with a pentobarbital overdose (100 mg/kg i.p.) and blood was withdrawn via the right ventricle for flow cytometry and biochemical analysis. Mice were perfused via the left cardiac ventricle with PBS containing sodium nitroprusside (0.1 mg/ml; Millipore). Aortic arch and organs of interest were dissected and fixed in 1% PFA overnight and paraffin-embedded. Aortic roots were serially sectioned and stained with hematoxylin and eosin (H&E) for plaque area and

necrotic core content. Five consecutive H&E sections at 20 μm intervals were analyzed blindly using computerized morphometry (Leica QWin V3) and averaged per mouse. A 100 μm interval where a fully developed media within the aortic valves was present was determined for each mouse. Sections within this 100 μm interval were used for immunohistochemical staining. Plaques were staged as early (intimal xanthoma), moderate (pathologic intimal thickening, PIT), or advanced (fibrous cap atheroma) as described before (17).Two sections per mouse were stained with Sirius Red for collagen quantification and averaged per mouse. Immunostaining for LAMP-2A in mouse aorta was performed using a rabbit anti-LAMP-2A (Thermo scientific; 512200) following standard procedures. Macrophages and VSMC were immunostained using rabbit anti-CD68 (ab125212, Abcam) antibody followed by secondary anti-rabbit HRP-labeled antibody (DPVR-55-HRP, Immunologic) and anti-αSMA (F3777, Sigma) followed by secondary-HRP-labelled antibody (11.426.346.910, Roche), respectively. Epitope-antibody binding was visualized as a brown precipitate using diaminobenzidine. Alizarin red (A5533-25G, Sigma) was used to detect calcification. For colocalization staining, primary antibodies, followed by secondary anti-rabbit AP-labelled antibody (DPVR-55-AP, Immunologic) were used in CD68 and LAMP-2A staining, and for VSMC staining mouse anti-αSMA (M0851, Dako) primary antibody, followed by secondary anti-mouse Biotin-labelled antibody (RPN1001v1, Amersham) and ABC-AP amplification (AK-5000, Vector) were used. Epitope-antibody binding was visualized as either blue or red precipitate using Vector substrate kits (SK-5300 or SK-51000, respectively).

Lipid analysis
Plasma was obtained by centrifugation at 6,000g for 10 min at 4°C, snap-frozen and stored at -80˚C until further use. Pooled plasma samples from mice according to genotype and treatment were used for lipoprotein fractioning on a Superose 6 PC 3.2/30 column (ÄAkta System, Amersham Pharmacia Biotech). The samples were eluted at a constant flow rate of 50 μl/min in PBS (pH 7.4). Fractions of 50 μl were collected and assayed for TC and TG using the kits described above. Plasma levels of insulin and PAI-1 were measured using ELISA (90080, Crystal Chemicals and ab197752, Abcam). Plasma levels of CCL3, CCL4 and G-CSF were measured using MILLIPLEX MAP Mouse Cytokine/Chemokine kit (Millipore) in a Luminex Magpix (Luminex).

Metabolic analysis
Body weight was measured weekly during the study period. Body composition was determined on 21-week-old mice by magnetic resonance spectroscopy (MRS) using an echo MRS instrument (Echo Medical System) and metabolic measurements (oxygen consumption, carbon dioxide production, food intake, and locomotor activity) were obtained continuously every 8 minutes using a CLAMS (Columbus Instruments) open-circuit indirect calorimetry system for 8 days. Insulin resistance was measured with an intraperitoneal insulin tolerance test (ITT) performed on 21-week-old mice after 4h fasting. Blood glucose was measured before i.p. of insulin (1.5 U/kg body weight) and then 15, 30, 45, 60, 90, 120 and 150 minutes after injection.

Flow cytometry and serum parameters
Whole blood cell composition was analyzed using flow cytometry after erythrocyte lysis and incubation with the following specific antibodies to detect leucocyte subsets: leucocytes (CD45+; 103129, Biolegend), T cells (CD3ε+, NK1-1-; 48-0032-80, ThermoFisher), T helper cells (CD4+; 15-0041-81, ThermoFisher), cytotoxic T cells (CD8a+; 11-0081-82, ThermoFisher), B cells (CD45R/B220+; 561227, BD), NK cells (NK1-1+; 561046, BD), granulocytes (CD11bhigh Ly6Ghigh; 11-0112-41 ThermoFisher, 560600, BD, respectively) and monocytes (CD11bhigh Ly6Glow Ly6Chigh/intermediate/low) using the Absolute Counting Tubes (340334, BD Trucount). Data were acquired using a Becton Dickinson LSRII-U and analyzed with FACSdiva software (BD) and gating strategy is depicted in **Supplementary Scheme 1**.

Human carotid plaque analysis
Human carotid autopsy samples (study 1) were processed for immunohistochemistry as follows. After antigen retrieval (target retrieval DAKO), slides were incubated overnight with primary antibody (Human LAMP-2A (ab18528, Abcam), CD68 (macrophage marker, ab125212, Abcam) or αSMA (VSMC marker, F3777, Sigma)), followed by secondary-biotin-labelled antibodies, and ABC-HP amplification (Vector). Epitope-antibody binding was visualized as a brown precipitate using diaminobenzidine. Colocalization of LAMP-2A and CD68 and αSMA was done on directly adjacent

sections using rabbit anti-LAMP-2A (18528, Abcam), mouse anti-CD68 (M0814, Dako) and mouse anti-αSMA (M0851, Dako) primary antibodies respectively, followed by either anti-mouse or anti-rabbit AP-labelled secondary antibody (DPVM-55-AP or DPVR-55-AP, Immunologic). Epitope-antibody binding was visualized as either a blue (LAMP-2A) or red (CD68/αSMA) precipitation using Vector substrate kits (SK-5300 or SK-51000 respectively).

LAMP-2A mRNA expression in thick fibrous cap atheromas and intraplaque hemorrhage-rich plaques was analyzed by microarray derived from paired segments of the same patient undergoing carotid endarterectomy (study 2) (10). LAMP-2A mRNA expression intensities from microarrays were correlated with morphometrically analyzed histological plaque characteristics: plaque size, necrotic core (% of plaque) and macrophages (% CD68 of plaque).

LAMP-2 protein expression in human atherosclerotic plaque was analyzed using the AtheroExpress Study biobank, in which plaques from patients undergoing carotid endarterectomy were obtained (study 4). Protein lysates of these plaques were used for western blot analysis and compared between groups with one event at baseline or a second event at follow up.

CMA activity

CMA activity *in vivo* was determined in aorta arches from KFERQ-Dendra2 mice using CT embedding method as following: Aortas were fixed for 12h at 4°C in fixation buffer (2% formaldehyde, 0.2% picric acid in PBS, pH7.0) and then washed with 70% ethanol, followed by two washes in PBS. Tissues were immersed in 30% sucrose and then embedded in OCT for sectioning in a cryostat (Leica CM3050 S). After air-drying for 30 min, sections were stored at -20°C until use. Colocalization of CD68 and αSMA was done on sequential serial sections using rat anti-CD68 (Bio-Rad, mca1957) and rabbit anti-αSMA (Abcam, ab202510, alexa 594-labelled). Slices were mounted in DAPI-Fluoromount-G to highlight the cell nucleus. Direct fluorescence images were obtained with a confocal microscope (TCS SP5; Leica) using an HCX Plan Apo CS 63.0× 1.40 NA oil objective in the Leica Application Suite X (LAS X) or an Olympus FV1000 multiphoton microscope with a 25× 1.05 NA water immersion objective as previously described(18). Collagen was visualized by second harmonic generation.

CMA activity in cultured VSMC was measured using lentivirus-mediated expression of fluorescent photoswitchable KFERQ-PSDendra2 reporter (19). Cells were photoswitched with a 405nm light emitting diode (LED: Norlux) for 3 min with 3.5mA (constant current) and 16 h later fixed with 1% paraformaldehyde. Images were acquired with an Axiovert 200 fluorescence microscope (Carl Zeiss), with 1.4 numerical aperture. The average number of fluorescent puncta per cell was quantified using Image J (NIH) in individual single planar images after thresholding. Values are presented as number of puncta per cell section that in our acquisition conditions represents 10-20% of the total puncta per cell (20).

Lysosomal isolation

Lysosomes were isolated from BMDM after disruption of the plasma membrane by nitrogen cavitation and sequential centrifugation in Percoll/metrizamide discontinuous density gradients (21). Preparations with more than 10% broken lysosomes, measured by β-hexosaminidase latency, were discarded (21).

Microarray

Total RNA from a pool of 3 independent experiments with VSMC in culture was extracted using TRIzol (Invitrogen) and purified with RNeasy chromatography (Qiagen) in LPDS media and LPDS plus LDL (150 μg/ml). Cy3-labeled RNA (0.6 μg) from each condition were hybridized to Agilent Mouse 8x60K. Data were processed using the oligo package and normalized using Robust Multiarray Average (RMA) method. Gene set was filtered to remove genes without Entrez or GO annotation (21912 genes out of 55682) and genes with an IQR > 0.5. The full microarray raw data has been deposited in GEO GSE143162. Pathway analysis was performed using the IPA software (Ingenuity Systems) and STRING database (https://string-db.org/).

Calculation of CMA score

Expression intensities (log) for every gene in the CMA network were preprocessed and normalized as described (22). First, to avoid dimensionality issue, each gene was centered and scaled across all patients. Then, for every patient (or cell type in scRNAseq data), a CMA score was calculated. by computing an eigengene, which is a weighted average expression over all genes in the

corresponding CMA network. To do so, each element of the CMA network (23) was attributed a *weight*. As LAMP-2A is the rate limiting component of CMA, it was given a *weight* of 2. Every other element received a *weight* of 1. Then, every element was attributed *direction* score that is +1 or -1 based on the known effect of a given element on CMA activity (22). The score was then calculated as the weighted/directed average of expression counts of every element of the CMA network. Higher scores, predictive of CMA activation, could result from (i) increased expression of effectors or positive modulators or (ii) decreased expression of negative modulators. Conversely, (i) decreased expression of effectors or positive modulators, or (ii) a higher expression of negative modulators will render lower CMA activation scores. CMA score calculation and plotting was done using Python (Python software foundation v.3.7.4 available at https://www.python.org/) and the scientific python stack: scipy (v.1.3.1), numpy (v.1.17.2), and matplotlib (v.3.1.1).

Quantitative Proteomics and Protein Pathway Analysis

BMDM lysosomes active for CMA were isolated from WT and L2AKO macrophages treated in CTRL or stimulated with IFNγ/LPS and treated or not (untreated) with 2 mM NH_4Cl and 100 μM leupeptin 12 hours before isolation. Lysosomes from three different sets were pooled and analyzed for purity, integrity, ponceau red electrophoretic patterning and enrichment in markers of CMA lysosomes by immunoblot. Quantitative proteomics analysis was performed in the two different genotypes under the four different conditions using isobaric tags for relative and absolute quantitation (iTRAQ) by Applied Biomics, Inc.. For each sample (10 μg of protein), the buffer was replaced with 0.5 M triethylammonium bicarbonate, pH 8.5, followed by reduction, alkylation, trypsin digestion, iTRAQ labeling, and sample clean-up according to the manufacturer's instructions (AB SCIEX). NanoLC was carried out using a Dionex Ultimate 3000 (Milford, MA). Tryptic peptides were loaded into a μ-Precolumn Cartridge and separated on an acetonitrile gradient (ranging from 5% to 60%) on a C18 Nano LC column. Fractions were collected at 20-second intervals followed by Mass Spectrometry analysis on AB SCIEX TOF/TOF™ 5800 System (AB SCIEX). Mass spectra were acquired in reflectron positive ion mode. TOF/TOF tandem MS fragmentation spectra were acquired for each ion, averaging 4,000 laser shots per fragmentation spectrum on (excluding trypsin autolytic peptides and other known background ions). The resulting fragmentation spectra were submitted to MASCOT search engine (version 2.3, Matrix Science) to search the database of National Center for Biotechnology Information non-redundant (NCBInr). Searches were performed without constraining protein molecular weight or isoelectric point, with variable methyl-thiolation of cysteine and oxidation of methionine residues, fixed N-terminal- and lysine-modifications with iTRAQ labels, and one missed cleavage. Quantitation was performed on peptides displaying an ion score confidence interval of 95 percent or higher.

For each protein hit the average ratio(s) for the protein, the number of peptide ratios that contributed, and the geometric standard deviation were determined. Values in the L2AKO untreated experimental groups were compared to their respective NH_4Cl/leupeptin treated samples and then with their respective WT groups and are represented as the average of folds (lysosomes isolated from untreated WT BMDM are given a value of 1). CMA substrate proteins were defined as those for which leupeptin treatment resulted in increase in lysosomal levels >10% and with a reduction in NH_4Cl/leupeptin response of >10% in the L2AKO. The protein sets catalogued as CMA substrates from the iTRAQ experiments were analyzed using the IPA software (Ingenuity Systems) and STRING database (https://string-db.org/).

Real-Time Quantitative-Polymerase Chain Reaction

Total RNA was isolated from cells using TRIzol Reagent (Invitrogen). RNA (1 μg) was used to perform the reverse transcription with High Capacity cDNA Archive Kit (Applied Biosystems). Real-time PCR reactions were performed on an ABI Prism 7500 sequence detection PCR system (Applied Biosystems) according to manufacturer's protocol, using the ΔΔCt method as described (24). Quantification of mRNA levels was done by amplification of cDNA using Power SYBR Green PCR Master Mix (4368702, ThermoFisher). The primer sequences are listed in **Table S6**. Expression levels are given as ratio to housekeeping gene HPRT1 and data is expressed as fold vs basal values.

Other methods

Rates of cellular proliferation were determined as incorporation of BrdU 24h after plating

(11444611001, Sigma) and cytotoxicity was determined by ApoTox-Glo Triplex Assay (G6320, Promega). Electrophoresis and immunoblot were performed using nitrocellulose membranes after cell lysis in 0.25M sucrose buffer (pH 7.2) containing protease and phosphatase inhibitors. Cell lysates were centrifuged at increasing speeds to discard intact cells (300 g, 10 min) and dead cells (2,000 g, 10 min). After electrophoresis and transfer to nitrocellulose membrane, the proteins of interest were visualized by incubation of the membranes with the primary and corresponding secondary antibody by chemiluminescence using peroxidase-conjugated secondary antibodies in G-BOX Chemi XX6 (Imgen). Red ponceau were used as loading control. Macroautophagy was measured upon transduction of cells with a lentiviral vector expressing mCherry-GFP-LC3 (25), as the conversion of dual fluorescence puncta (autophagosomes) into only red fluorescent puncta (autolysosomes). Immunoblot for LC3 and P62/SQSTM1 in cells incubated for 12h with NH_4Cl/leupeptin was used to analyze macroautophagy flux.

Statistical analysis

All data are presented as individual values (symbols) and/or mean+SEM For *in vitro* assays we determined the number of experimental repetitions to account for technical variability and changes in culture conditions. In all instances, “n” refers to individual experiments or animals. Data comes from a minimum of three independent experiments and instances with higher number of repetitions are indicated in the figure legends. The number of animals used per experiment was calculated through power analysis based in previous results. Animals were randomly attributed to control or treatment groups. No mouse was excluded from the analysis unless there were technical reasons, or the mouse was determined to be in very poor health by the veterinarian. Outliers were determined by the ROUT method (Q=1%). Investigators were blinded to the treatment during data collection and analysis and unblinding was done when the analysis was completed for plotting. If not indicated otherwise, all parameters were analyzed using independent sample tests and were tested for normal distribution using D’Agostino & Pearson normality test. Parameters with two groups were compared with student’s t-test or Mann-Whitney rank-sum test, depending on outcome of the D’Agostino & Pearson normality test. In case of more than two groups, parameters were analyzed using two-way ANOVA followed by Bonferroni’s Multiple Comparison Test or Kruskal-Wallis rank-sum test, followed by Dunn’s post-hoc testing, in the absence of a normal distribution. CMA activity measured by KFERQ-Dendra2 puncta in VSMC was subjected to Analysis of Variance (One-way ANOVA) followed by Tukey’s post hoc tests. Time course experiments were analyzed using repeated measured (mixed model) ANOVA, followed by Bonferroni post-tests upon confirmation of homogeneity of variances using Levene’s (GraphPad 7.0). Human plaque analysis. Correlation analysis was performed using Spearman bivariate correlation analysis (IBM SPSS statistics 22). Human plaque L2A levels were significantly skewed, thus square root transformation normalized the distribution. As L2A levels were significantly different between male and females, we performed sex-stratified logistic regression analysis of the association of the incidence of a second cardiovascular event with stepwise, forward inclusion (wald) of square-root transformed L2A, age, hypertension and BMI (n=22 females, 37 males). Also, the sex-stratified associations of square-root transformed L2A, age, hypertension and BMI with time to a second event were analysed using cox regression. Analysis was done with IBM SPPS statistics (version 25).

Materials availability

All reagents generated in this study are available from the Lead Contact with a completed Material Transfer Agreement.

Data and code availability

There are no restrictions on data availability in this manuscript. All the information is included in the manuscript. All Main and Supplementary Figures have associated raw data that is provided as an Excel worksheet organized by figures and it includes statistics along with exact p values. The full microarray raw data has been deposited in GEO accession number GSE143162. This manuscript does not report original code.

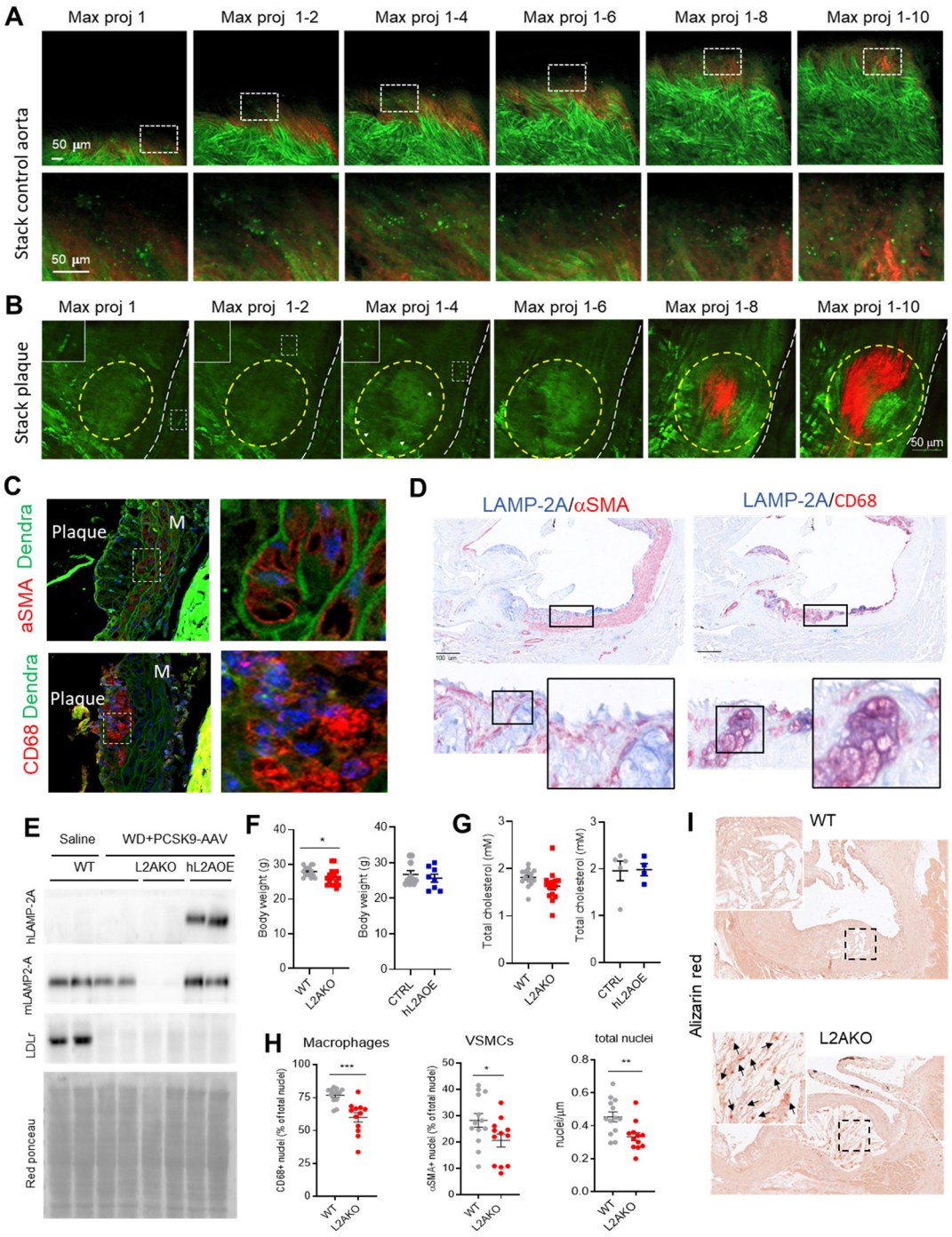

Figure S1. Characterization of the mouse models used in this study. (A,B) Representative images of aortas from KFERQ-Dendra2 mice untreated (Control, A) or subjected to a pro-atherosclerotic treatment (injected with AAV8 PCSK9 and maintained for 12 weeks on the Western-type diet) (B). Sequential maximal projections are shown. Insets show boxed area at higher magnification. In B the plaque region is denoted by the circle and identified by the accumulation of collagen (red). (C) Aorta sections containing atherosclerotic plaques from the KFERQ-Dendra2 mice in B, co-stained with α-SMA or CD68. Insets on right show boxed area at higher magnification. M: media. Experiments in

A-C were repeated 3 times with similar results. (D) Representative images of the colocalization of LAMP-2A with αSMA (left) and CD68 positive cells (right) in a murine atherosclerotic plaque. (E) Immunoblot for human LAMP-2A (hLAMP-2A), murine LAMP-2A (mLAMP-2A) and LDLR in livers from wild type (WT), LAMP-2A null mice (L2AKO) and mice systemically expressing a copy of human LAMP-2A (hL2AOE) injected retro-orbitally with saline or AAV8-PCSK9 as indicated. Ponceau red is shown as loading control. (F,G) Basal metabolic parameters in WT, L2AKO and hL2AOE mice at 3 months of age. Body weight (F) and total cholesterol levels (G). (n=15 WT, n=16 L2AKO (in F and G) and n=10 CTR and n=8 hL2AOE (in F) and n=5 CTRL, n=4 hL2AOE (in G). (H) Total number of nuclei (right) and percentage of macrophages (left) and VSMCs (middle) in plaques from wild type (WT) and LAMP-2A null mice (L2AKO) subjected to the pro-atherosclerotic challenge for 12 weeks. (I) Representative images of Alizarin red staining of aorta from WT and L2AKO mice subjected to the pro-atherosclerotic intervention. Insets: boxed area at higher magnification. Arrows: calcium deposits. Quantification is shown in Figure 1R. All data, when applicable, were tested for normal distribution using D'Agostino and Pearson normality test. Variables that did not pass normality test were subsequently analyzed using Mann–Whitney rank-sum test. All other variables were tested with the Student's t-test. Individual values (symbols) and mean ± SEM are shown. *p <0.05, **p <0.01 and ***p<0.001.

A

	WT	L2AKO	p-value
Liver (mg/mm)	6.62 ± 0.19	9.69 ± 0.47	****
eWAT (mg/mm)	3.66 ± 0.31	6.79 ± 0.75	***
Kidneys (mg/mm)	1.81 ± 0.05	1.78 ± 0.1	ns
Feces (g/day)	0.23 ± 0.016	0.19 ± 0.011	*

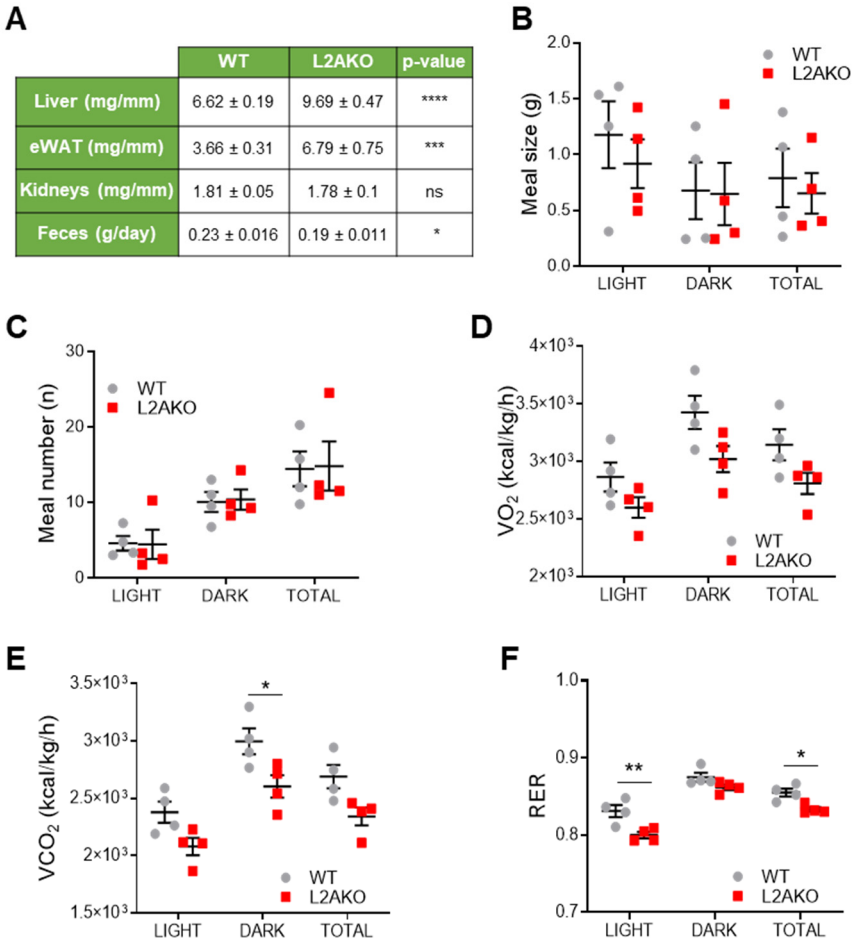

Figure S2. Metabolic profile of CMA deficient mice subjected to an experimental model of murine atherosclerosis. (A) Tissue weights after 12 weeks of Western-type diet in wild-type (WT) (n=15) and LAMP-2A null mice (L2AKO) (n=14). Tissue weights are normalized by tibial length and expressed as mean ± SEM. (B-F) Metabolic parameters measured by indirect calorimetry in WT and L2AKO mice fed a Western-type diet for 6 weeks: Meal size (Meal size: two-way ANOVA, F = 0.1027; P = 0.9029 for interaction, F = 1.359; P = 0.2820 for light/dark/ total, F = 0.4767; P = 0.4987 for genotype, n=4) (B), meal number (Meal number: two-way ANOVA, F = 0.01; P = 0.99 for interaction, F = 12.83; P = 0.0003 for light/dark/ total, F = 0.0122; P = 0.9133 for genotype, n=4) (C), volume of O_2 consumption ambulatory parameters (VO2: two-way ANOVA, F = 0.1759; P = 0.8401 for interaction, F = 8.587; P = 0.0024 for light/dark/total, F = 12.04; P = 0.0027 for genotype, n=4) (D), volume of CO_2 production (VCO2: two-way ANOVA, F = 0.1254; P = 0.8829 for interaction, F = 18.38; P < 0.0001 for light/dark/total, F = 20.33; P = 0.0003 for genotype, n=4) (E) and RER (RER: two-way ANOVA, F = 1.537; P = 0.2419 for interaction, F = 54.04; P < 0.0001 for light/dark/ total, F = 27.8; P < 0.0001 for genotype, n=4) (F). All data were tested for normal distribution using D'Agostino and Pearson normality test. Variables that did not pass normality test were subsequently analyzed using Mann–Whitney rank-sum test. All other variables were tested with the Student's t-test. ns indicates p-value=non-significant. Graphs represent individual values, mean ± SEM. *p <0.05 and **p <0.01.

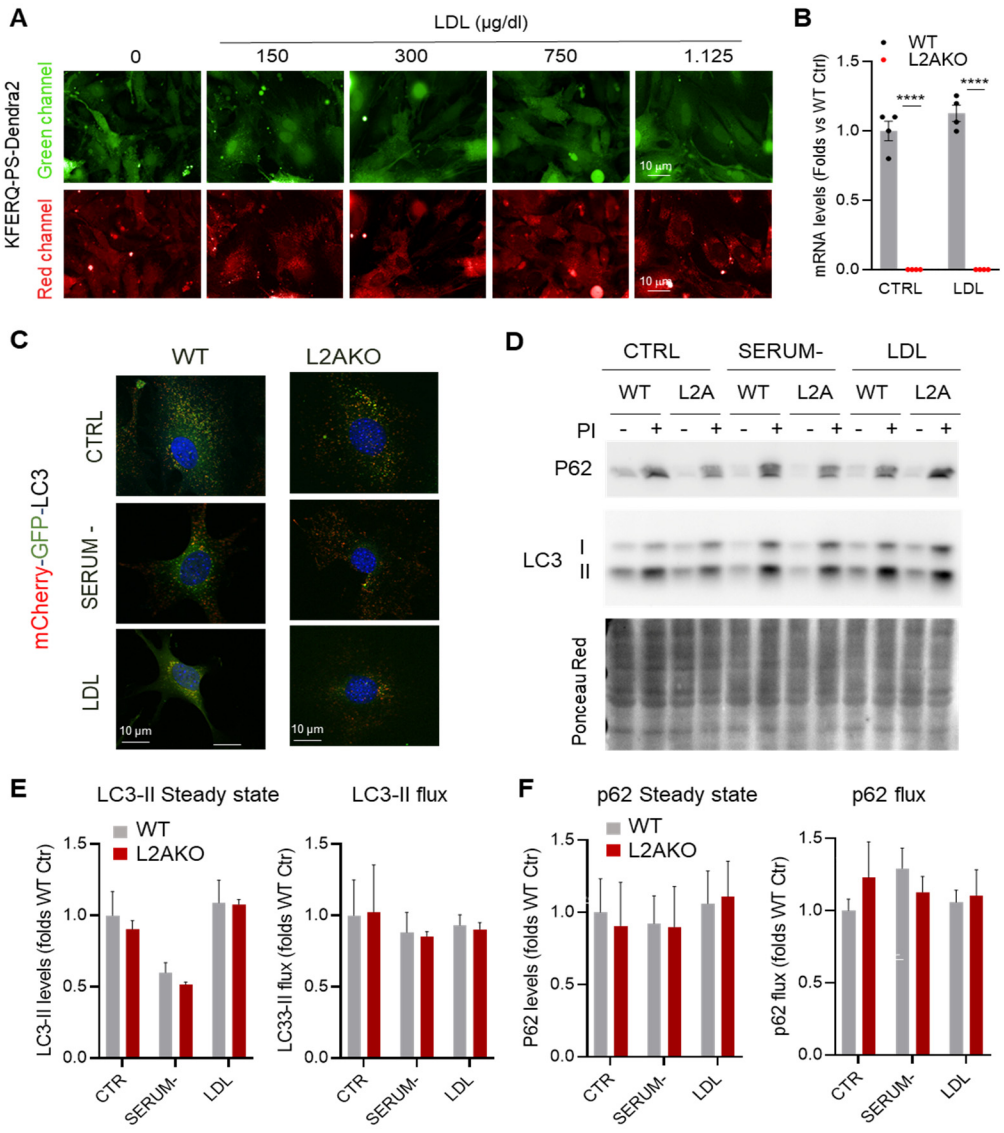

Figure S3. Autophagic changes in VSMC upon lipid challenges. (A) CMA activity in murine VSMC stably expressing the KFERQ-PS-Dendra2 CMA reporter and challenged with the indicated concentrations of LDL. Representative images of separate channels. Quantification is shown in Figure 3A. (B) LAMP-2A mRNA in VSMC cells isolated from WT and L2AKO mice and exposed to the indicated lipid challenge. n=4 isolations from 4 independent mice per group. (C) Macroautophagy flux detected by direct fluorescence in WT and L2AKO VSMC transfected with the tandem reporter mCherry-GFP-LC3. Representative images of merged channels are shown. Nuclei are highlighted with DAPI. The experiment was repeated 4 times with similar results. (D-F) Immunoblot for LC3-II and P62/SQSTM1 in WT and L2AKO VSMC under the indicated conditions. Macroautophagy flux is detected as an increase in LC3-II and p62 intensity upon inhibition of lysosomal hydrolysis with protease inhibitors (PI). Ponceau red was used as loading control. Quantification of steady state (left) and flux (right) for LC3-II (E) and p62 (F) from the densitometric analysis of blots as the ones shown in D from n =3 independent experiments. Values are mean+s.e.m. ****p<0.001

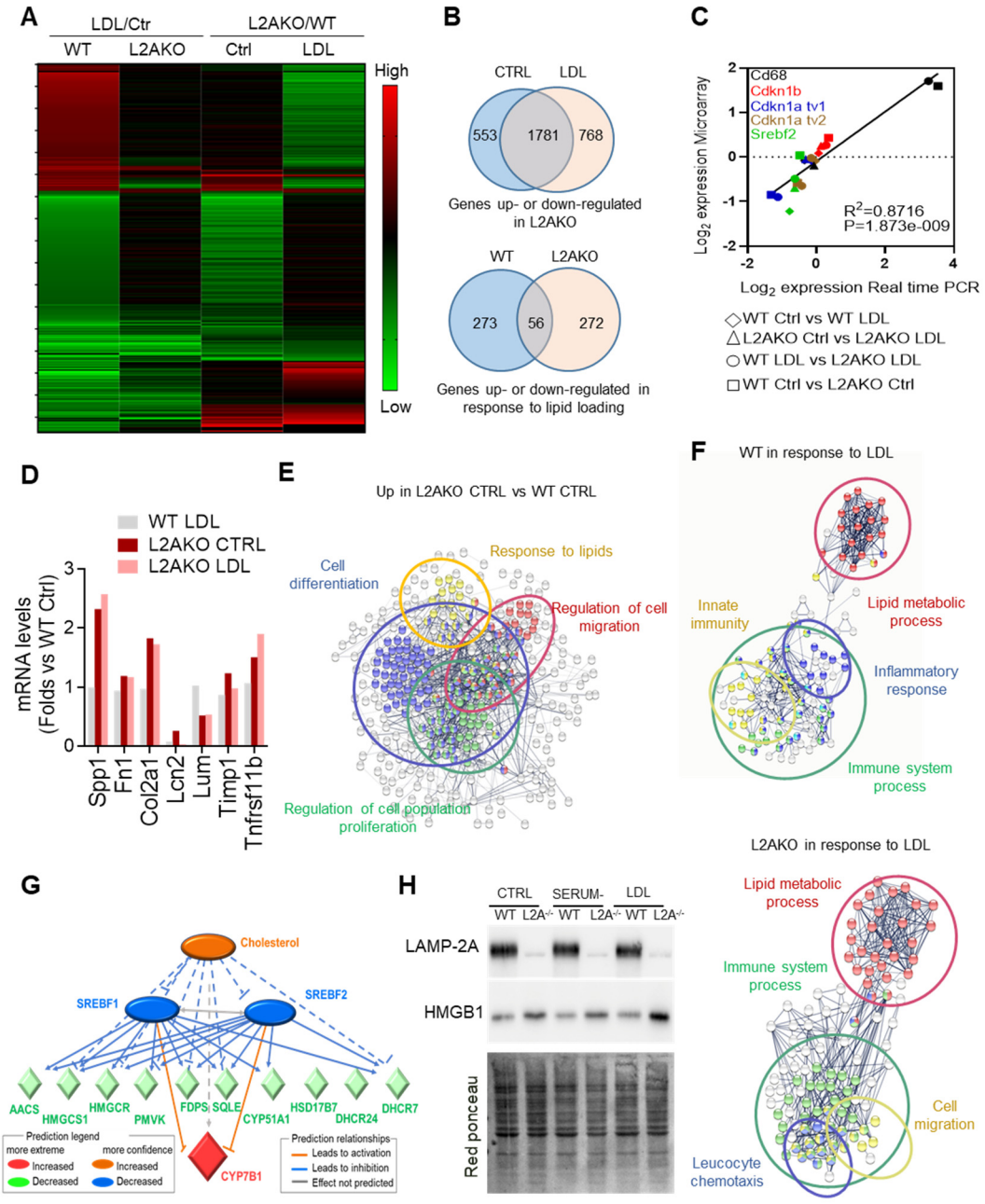

Figure S4. Differential transcriptional and protein profile of CMA-deficient VSMC. (A) Hierarchical heatmap of transcriptional changes (Log2 fold) in VSMC from wild type (WT) and LAMP-2A null mice (L2AKO) cultured under basal conditions (control, CTRL) or upon LDL loading. (B) Venn diagrams showing the number of genes upregulated and downregulated (cutoff >± 1 log_2 fold change) WT and L2AKO VSMC in basal conditions (top) or in response to LDL treatment (bottom) compared to the same conditions in the WT cells. (C) Validation by RT-PCR of selected genes identified in the microarray in three independent experiments and to *Hprt1* expression. Scatter plot showing the significant positive relationship between selected mRNA gene expression obtained by microarray and RT-PCR. Level of significance was determined by Pearson correlation. R^2=0.8716; P=1.873e-09. (D) Changes in mRNA levels of genes recently identified as markers of

modified dedifferentiated VSMC (12) in primary WT and L2AKO VSMC stimulated with LDL or maintained in a LPDS (CTRL) (pool of 3 individual experiments). (E,F) STRING analysis for pathways upregulated in L2AKO cells under basal conditions (E) or changing in response to LDL loading (F) in WT (top) or L2AKO VSMC (bottom). (G) Cholesterol biosynthetic network identified as one of the top networks of genes modulated differentially in WT and L2AKO primary VSMC. Red: increase, green: decrease. (H) Representative immunoblot for HMGB1 in cellular lysates of WT and L2AKO primary VSMC maintained in basal conditions or upon serum removal (-) or LDL loading. The experiment was repeated 3 times with similar results. All GEO terms are significant for $p<0.01$.

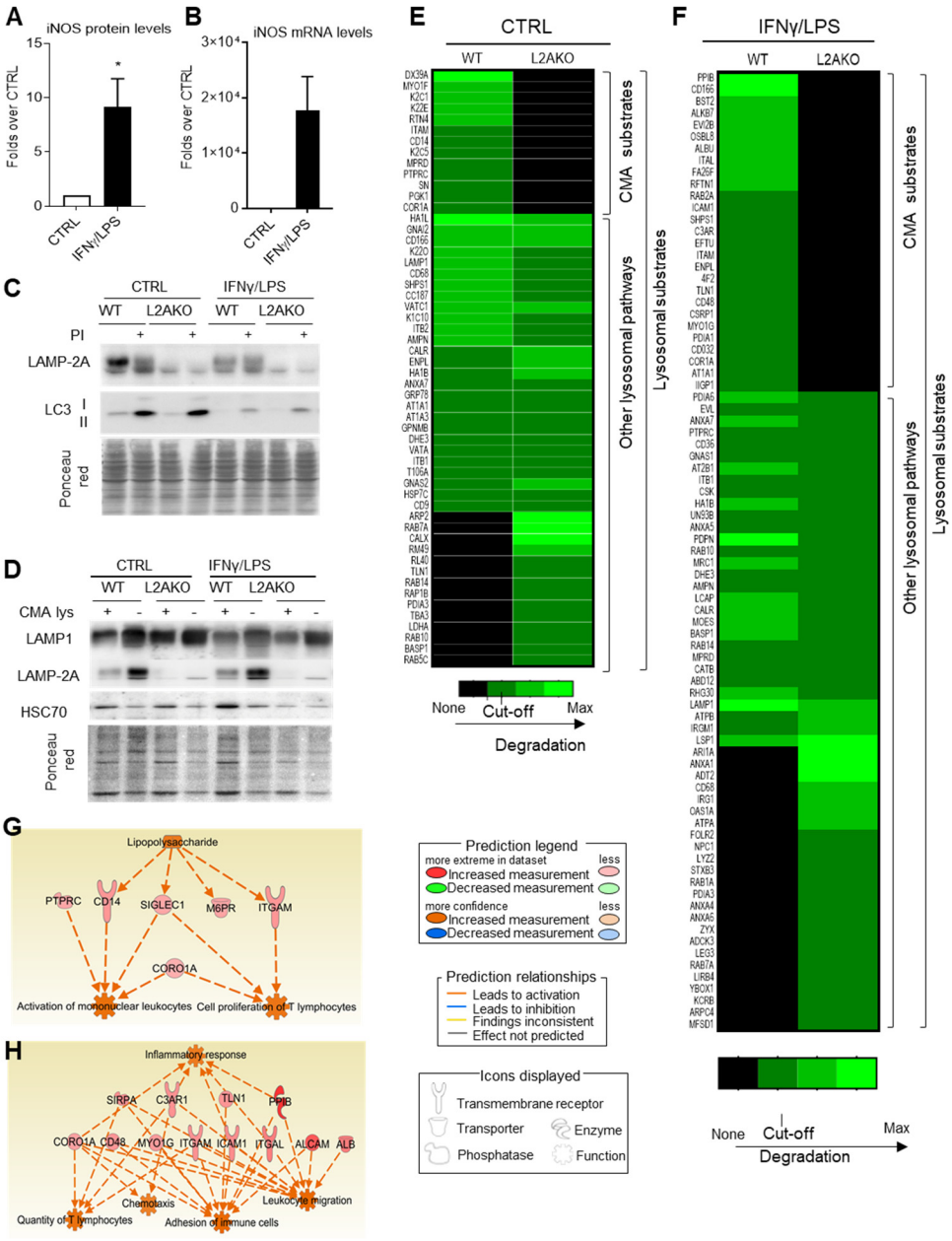

Figure S5. Characterization of CMA-deficient macrophages. (A,B) Levels of iNOS protein (A) and mRNA (B) in BMDM from wild type (WT) mice cultured without additions (control, CTRL) or stimulated with IFNγ/LPS. n=4. (C) Macroautophagy flux detected by immunoblot for LC3-II in WT and L2AKO BMDM control of or stimulated with IFNγ/LPS, detected as an increase in LC3-II intensity upon inhibition of lysosomal hydrolysis with protease inhibitors (PI). Ponceau red was used as loading control. The experiment was repeated 2 times with similar results. (D) Representative immunoblot for the indicated lysosomal components (LAMP1, LAMP-2A and HSC70) in lysosomes with high (+) or low (-) activity for CMA isolated from WT or L2AKO mouse BMDM. Ponceau red is shown as loading control. The experiment was repeated 3 times with similar results. (E,F) Heat map of changes in levels of the proteome of lysosomes from WT or L2AKO mouse BMDM CTRL (E) or exposed to IFNγ/LPS (F) upon inhibition of lysosomal proteolysis. (G,H)

Predicted activation in BMDM L2AKO cells of the LPS pathway due to accumulation of CMA substrates (G) and the inflammatory response in IFNγ/LPS treated cells (H) using the IPA software. All data, when applicable, were tested for normal distribution using D'Agostino and Pearson normality test. Variables that did not pass normality test were subsequently analyzed using Mann–Whitney rank-sum test. All other variables were tested with the Student's t-test. Graphs represent mean ± SEM. *p <0.05.

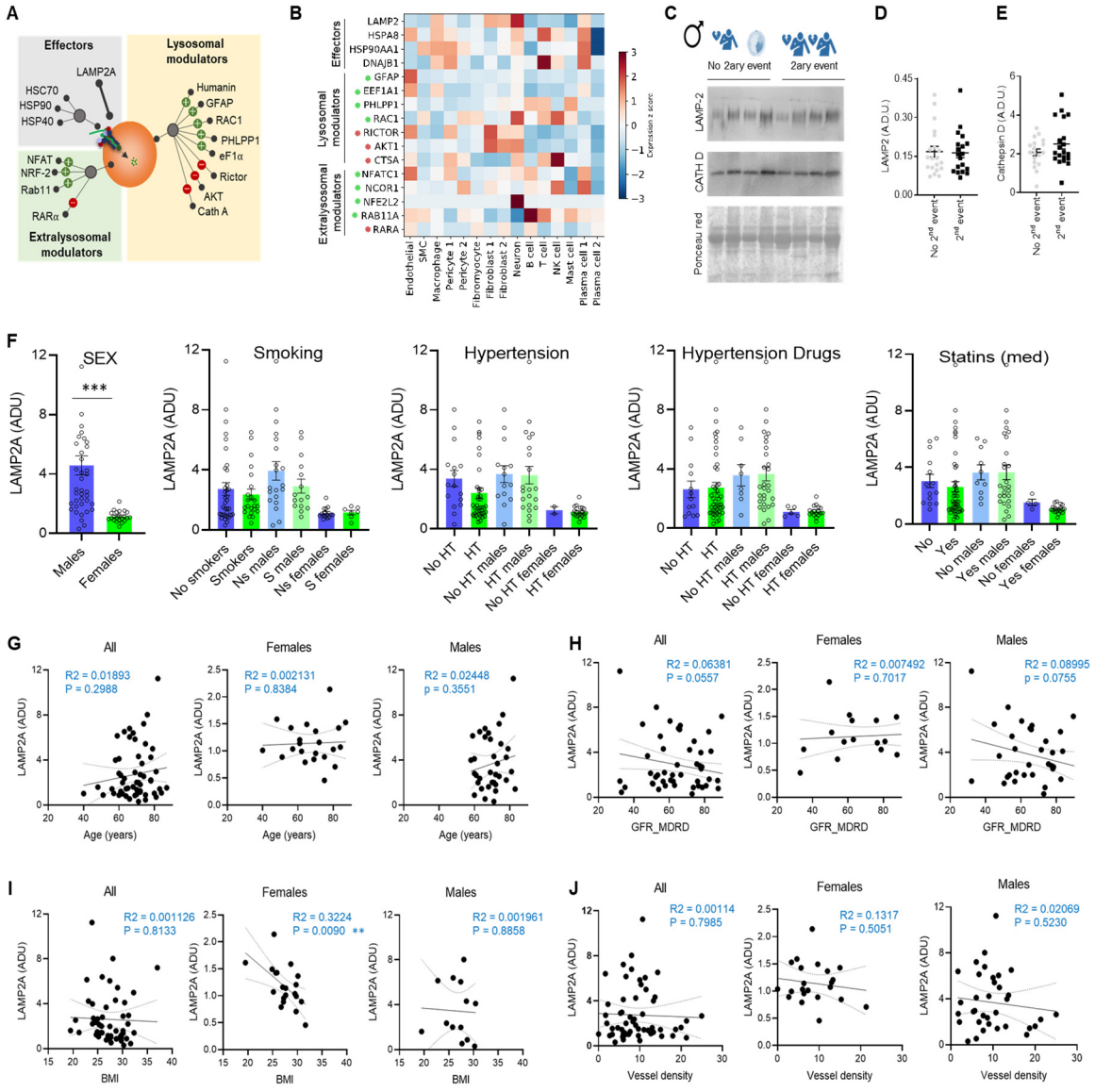

Figure S6. Changes in CMA components in carotid from atherosclerosis patients. (A) Schematic representation of the CMA network. Proteins involved in CMA are grouped based on function (effectors and modulators) and localization (lysosomal and extra-lysosomal). (Diagram modified from (Kirchner et al., 2019)). (B) Normalized expression (within each cell type) of individual component of the CMA network in scRNAseq from atherosclerotic plaques. CMA network elements are organized in functional groups and colored dots indicate the effect of a given element on CMA activity (Green: positive element; Red: negative element). (C-E) Protein levels for LAMP2 and Cathepsin D in plaque lysates from male patients who underwent a secondary coronary event (2nd event) or not (no 2nd event) subjected to immunoblot. Representative immunoblot (C) and individual and mean values of the densitometric quantifications for LAMP2 (D) and cathepsin D (E) are shown as arbitrary densitometric units (A.D.U.). Ponceau red is shown as loading control. (F) L2A expression levels in subcategories of clinical parameters, stratified by sex. (G-J) Correlation scatterplots of L2A levels with age, BMI, glomerular fitration rate (GFR) as indication of diabetes and vessel density independent (all) or

stratified by sex. All data, when applicable, were tested for normal distribution using D'Agostino and Pearson normality test. Variables that did not pass normality test were subsequently analyzed using Mann–Whitney rank-sum test. All other variables were tested with the Student's t-test (D, E), one way ANOVA (F) or simple linear regression with R^2 and p values indicated in blue (G-J). Individual patient values and mean ± SEM (D-F) or linear regression (G-J) are shown. n=62.

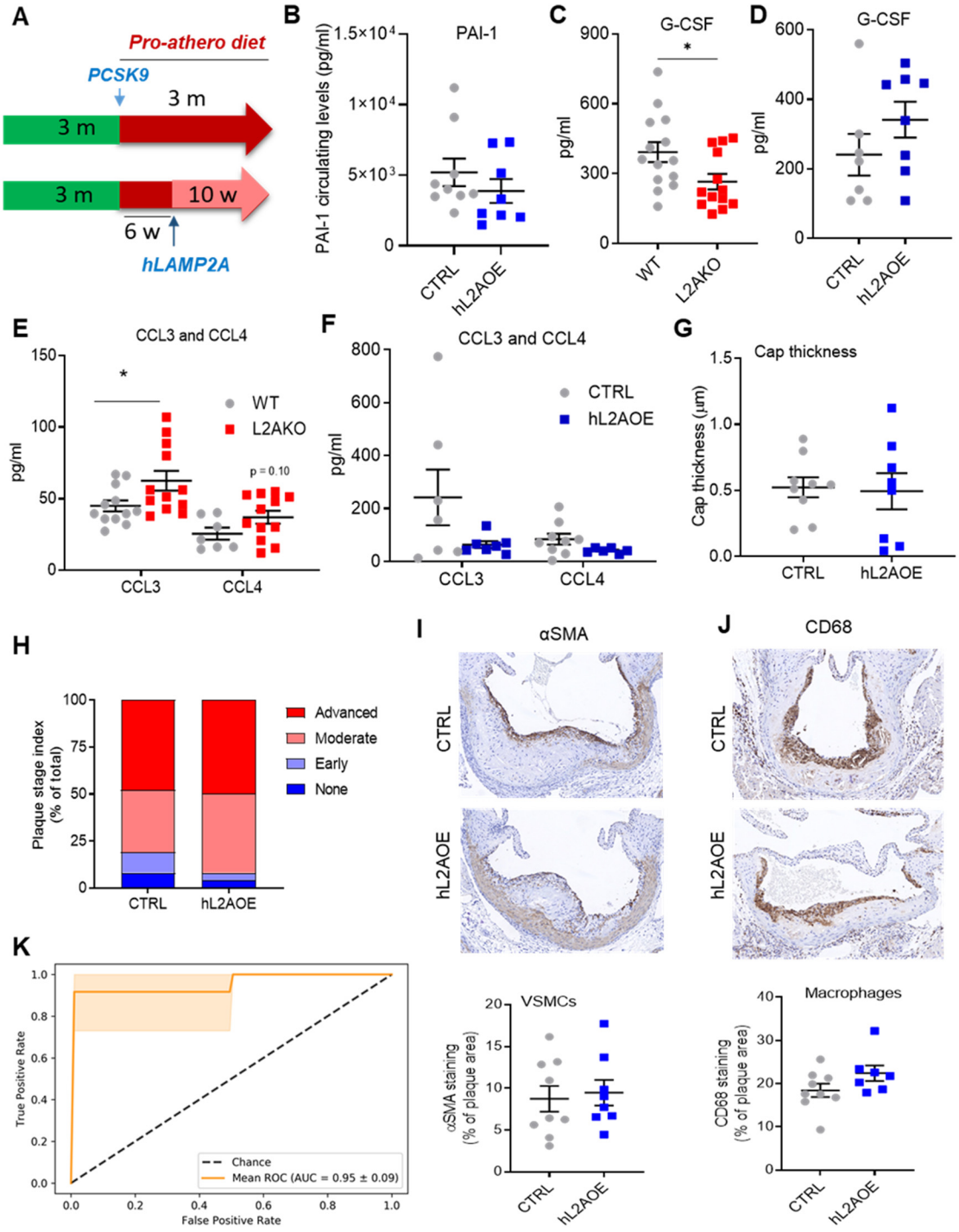

Figure S7. Characterization of mice with genetic upregulation of CMA subjected to an experimental model of murine atherosclerosis. (A) Scheme of the intervention to induce atherosclerosis (pro-athero) in mice systemically expressing a copy of human LAMP-2A (hL2AOE). (B-F) Levels of circulating PAI-1 (B), G-CSF (C,D) and CCL3 and CCL4 (E,F) in control (n=9) and hL2AOE (n=8) mice (B,D,F) and in wild-type mice (WT, n=15) and mice systemically null for LAMP-2A (L2AKO, n=14) (C,E). (G-J) Properties of the plaques from aortas of CTR and hL2AOE mice subjected to the pro-atherosclerotic

intervention. Quantification of cap thickness (G), plaque stage (H) and representative images (top) and quantification (bottom) of aortas immunostained for αSMA+ VSMC (I) and CD68 macrophages (J) Individual values (symbols) and mean ± SEM are shown. n=9 CTRL, n=8 hL2AOE. (K) Receiver operating characteristic curve showing the performance of a support vector machine with linear kernel trained to classify animals between CTRL and hL2AOE groups. Orange line represents the mean performance over 5 folds cross validation. AUC: area under the curve, ROC: receiver operating characteristics. All data, when applicable, were tested for normal distribution using D'Agostino and Pearson normality test. Variables that did not pass normality test were subsequently analyzed using Mann–Whitney rank-sum test. All other variables were tested with the Student's t-test. Graphs represent mean ± SEM. *p <0.05.

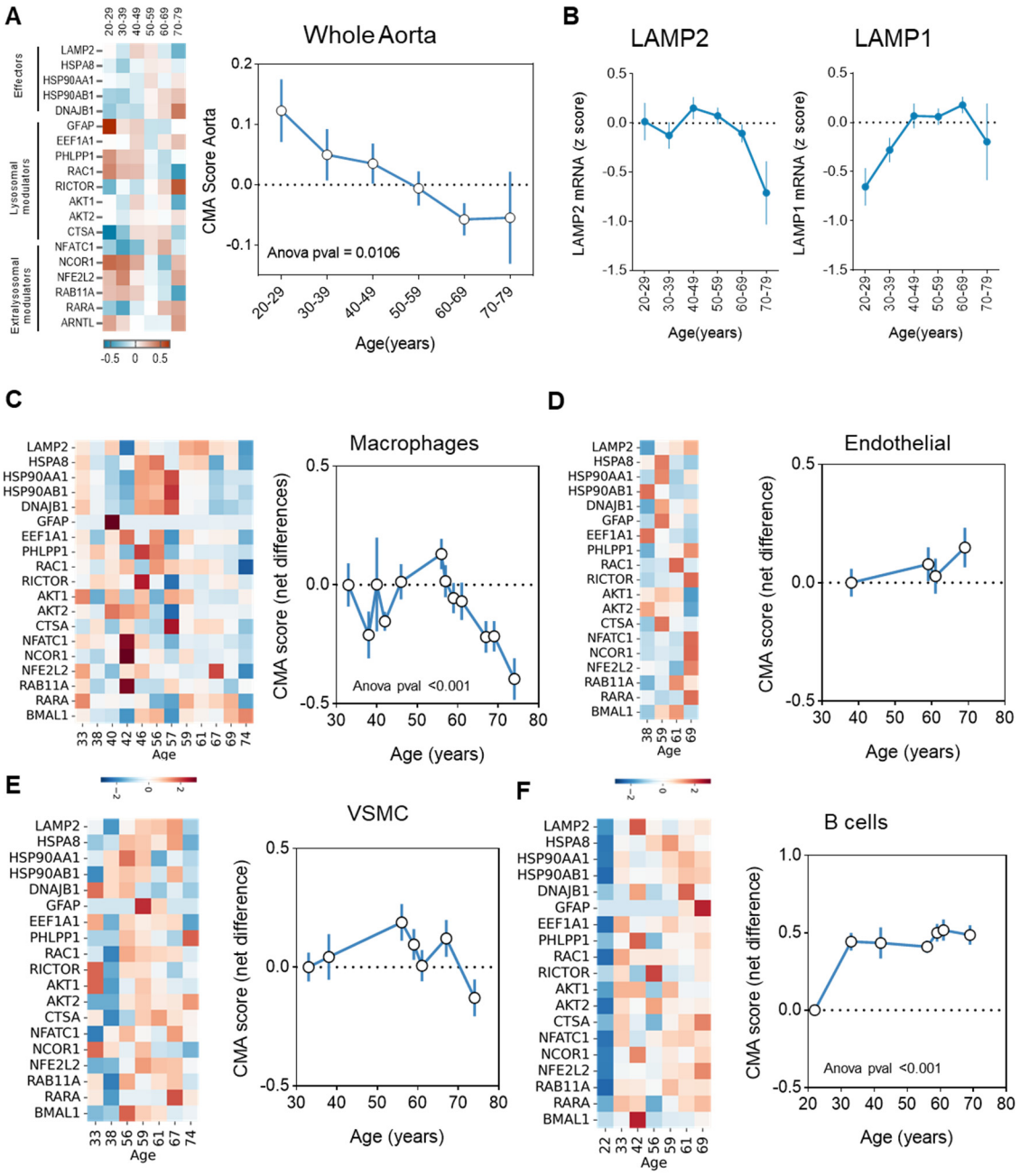

Figure S8. Changes in CMA with age in human vasculature. (A, B) Normalized expression of the CMA network components (left) and CMA activation score (right) (A) and LAMP2 and LAMP1 mRNA levels (B) in aorta from healthy individuals at the indicated ages calculated from RNAseq data in the GTEx aging database n=432 total samples (37, 38, 68, 149, 131 and 9 subjects for each age group shown, respectively). (C-F) Normalized expression of the CMA network components (left) and CMA activation score (right) expressed as net differences in the indicated cell types calculate from snRNAseq data in the Tabula Sapiens Consortium repository obtained from aortas of healthy subjects at the indicated ages. n=5-13. Graphs represent mean ± SEM. One-way ANOVA test was applied and p values are indicated in the graphs.

Table S1. Blood leucocyte profile in CMA deficient mice in a Western-type diet.

	WT	L2AKO	p-value
CD45+ leucocytes	9013 ± 378	9825 ± 620	ns
B220+ B cells	3825 ± 196	3273 ± 2931	ns
NK.1.1+ NK cells	193 ± 24	160 ± 10	ns
NK.1.1 low CD3low NK T cells	25.7 ± 3.9	21.5 ± 2.1	ns
NK.1.1 low CD3low CD4+ NKT CD4 cells	3.43 ± 0.68	2.91 ± 0.31	ns
NK.1.1 low CD3low CD8+ NKT CD8 cells	5.28 ± 0.78	5.84 ± 0.48	ns
NK.1.1- CD3- Non NK T cells	7250 ± 327	7596 ± 474	ns
CD11B+ Ly6G+ Granulocytes	1238 ± 84	1705 ± 113	***
CD11B+ Ly6C- Monocytes	1237 ± 107	1729 ± 144	*
CD11B+ Ly6C- Low inflammatory monocytes	680 ± 70	714 ± 61	ns
CD11B+ Ly6C Med Monocytes mid-inflammatory	152 ± 11	174 ± 15	ns
CD11B+ Ly6C High inflammatory monocytes	396 ± 40	832 ± 81	****
CD3+ Total T cells	1421 ± 75	1902 ± 145	**
CD3+ CD4+ TCD4 cells	707 ± 43	879 ± 55	*
CD3+ CD8+ TCD8 cells	617 ± 35	760 ± 46	*
CD3+ CD8+ Ly6C high Tmem cells	302 ± 22	336 ± 21	ns

Blood leukocyte count in wild type (WT) mice and mice systemically knocked out for LAMP-2A (L2AKO) maintained on a Western-type diet (n=15 WT and n=16 L2AKO)**.** All data are expressed as counts/µl and were tested for normal distribution using D'Agostino and Pearson normality test. Variables that did not pass normality test were subsequently analyzed using Mann–Whitney rank-sum test. All other variables were tested with the Student's t-test. Graphs represent mean ± SEM. *p <0.05, **p <0.01, ***p <0.005 and ****p <0.0001. ns=nonsignificant.

Table S2. Sources of human data/samples utilized in this work

	STUDY	Source	Type of patient	Artery	Data	Ref.	Panel
ATHEROSCLEROSIS	1	Autopsy	Deceased, no cardiovascular symptoms	Carotid artery	Histology of different plaque types (n=7-12 per group). Anonymize data	This work	5A-D, H
	2	Surgery, CEA	Symptomatic patients	Carotid artery	Microarrays of paired, intraplaque comparison of plaque segments with and without IPH, with quantified plaque traits in adjacent histological segments (n=36)	Jin et al, 2021	5E-G, L,M
	3	Heart transplants	Healthy donors, no cardiovascular symptoms	Coronary artery	Single cell sequencing of 4 human plaques. No histology	Wirka et al. 2019	5I
	4	Surgery, CEA	Symptomatic patients	Carotid artery	Prospective, 3-year follow-up study of recurring CV events with plaques collected at first event, and segmented for histology of plaque traits, and serial segments used for protein analysis.	Hellings et al, 2010	5J,K

	STUDY	Source	Type of patient	Sample	Data	Ref.	Panel
AGING	A1	GTEx portal	Healthy human subjects of different age groups	Aorta	RNAseq from artery aorta of individuals in the second (n=37), third (n=38), fourth (n=68), fifth (n=149), sixth (n=131) and seventh (n=9) decade of life.	Lonsdale et al. 2013	S8A, B
	A2	Tabula Sapiens	Normal human subjets (2 individuals with coronary artery disease were eliminated from the analysis)	Aorta	Single cells RNAseq of aorta (n=13, age range 22-79 years, 52% males). Specific donor characteristics in https://tabula-sapiens-portal.ds.czbiohub.org/whereisthedata	Tabula Sapiens, 2021	S8C-F

Table S3. Clinical - and plaque characteristics of the patients in study 4

Characteristic	Single event (n=34)	Recurrent event (n=28)
Age (years, mean ± SD)	65.3 ± 1,8	72.3 ± 1,4*
Sex (% males)	60.7	67.6
Current or prior smoking (%)	38.5	38.2
Arterial hypertension (%)	59.3	84,8*
Body Mass Index	26.9 ± 0,5	27.4 ± 0.7
eGFR MDRD, (mL/min/1.73 cm^2)	76.3 ± 3.1	66.2 ± 3.5*
Diabetes mellitus (%)	17.9	29.4
Medication lipid-lowering (%)	75	76.5
Medication anti-hypertensive (%)	71.4	85.3
Medication anti-platelet (%)	96.4	91.2
Medication anti-coagulant	7.1	17.6
PAOD history	35.7	32.4
Stroke history	14.3	26.5
CAD history	28.6	35.3
Stenosis contralateral (%)	29.6	53.1
Plaque phenotype		
Intraplaque hemorrhage (%)	71.4	79.4
Macrophage content (yes %)	53.6	52.9
smooth muscle content (yes %)	75.0	72.7
Collagen (yes %)	75.0	75.8
Calcification (yes %)	60.7	64.7
Lipid content (yes %)	85.7	73.5

* P-value < 0.05 single vs. recurrent event, T-test for continuous variables, Fisher's exact test for binary variables mean ±SEM. dGFR, estimated glomerular filtration rate; MDRD, Modification of Diet in Renal Disease.PAOD, Peripheral Arterial Occlusive Disease Clinical Presentation

Table S4. Association of LAMP2A with risk of recurrent event at 3 year follow-up stratified for sex

Gender	Parameter	B	S.E.	Wald	df	Sig.	Exp(B)
Female*	LAMP2A	-10,475	5,298	3,910	1	,048	,000
	Constant	10,877	5,550	3,841	1	,050	52942,6
Male**	Age	,29	,10	8,97	1	,003	1,3
	Hypertension	2,16	1,11	3,80	1	,051	8,7
	Constant	-21,04	6,98	9,09	1	,003	,000

Logistic regression analysis with forward, stepwise inclusion (wald) of square-root transformed L2A, age, hypertension and BMI stratified by gender (n=22 females, 37 males). * -2 Log likelihood=19,2; Cox & Snell R Square 0,31, Nagelkerke R Square 0,42; ** -2 Log likelihood=26,9 ; Cox & Snell R Square 0,43, Nagelkerke R Square 0,56.

Table S5 Cox regression analysis of L2A with time to recurrent event within 3 year follow-up stratified for sex

Gender	Parameter	B	S.E.	Wald	df	Sig.	Exp(B)
Female*	LAMP2A	-6,986	2,95	5,6	1	,018	,0
	Age	,001	,04	,0	1	,987	1,0
	Hypertension	13,024	814,98	,0	1	,987	453348,9
Male**	LAMP2A	-,007	,331	,000	1	,983	1,0
	Age	,154	,043	12,623	1	,000	1,2
	Hypertension	,532	,549	,938	1	,333	1,7

Cox regression analysis with time to recurrent event and square-root transformed L2A, age, and hypertension stratified by gender (n=22 females, 37 males).* -2 Log likelihood=37,43. **-2 Log likelihood=94,02.

Table S6. List of primers for murine samples used in this study.

Gene	*Forward primer*	*Reverse primer*
Cd68 (tv 1)	*GGACCGCTTATAGCCCAAGG*	GGATGGCAGGAGAGTAACGG
Cdkn1a *(tv 1)*	CGGTGTCAGAGTCTAGGGGA	GCCTGTGGCTCTGAATGTCT
Cdkn1a *(tv 2)*	TGGAGACAGAGACCCCAGAT	CAGGATTGGACATGGTGCCT
Cdkn1b	*CAGACGTAAACAGCTCCGAATTA*	*ACACAGGTAGTACAACAAAGCAA*
Hprt1	*ACAGGCCAGACTTTGTTGGA*	*ACTGGCAACATCAACAGGACT*
Ptgs2 (Cox2)	*CTTCGGGAGCACAACAGAGT*	*AAGTGGTAACCGCTCAGGTG*
Lamp-2 (Lamp-2a, tv 1)	*CTTAGCTTCTGGGATGCCCC*	*GCACTGCAGTCTTGAGCTGT*
Nos2 (iNOS)	*TCCTGGACATTACGACCCCT*	*AGGCCTCCAATCTCTGCCTA*
Srebf2	*GTCTCCCTGAGCTGGACCT*	*TAGCATCTCGTCGATGTCCC*

Tv: transcript variant.

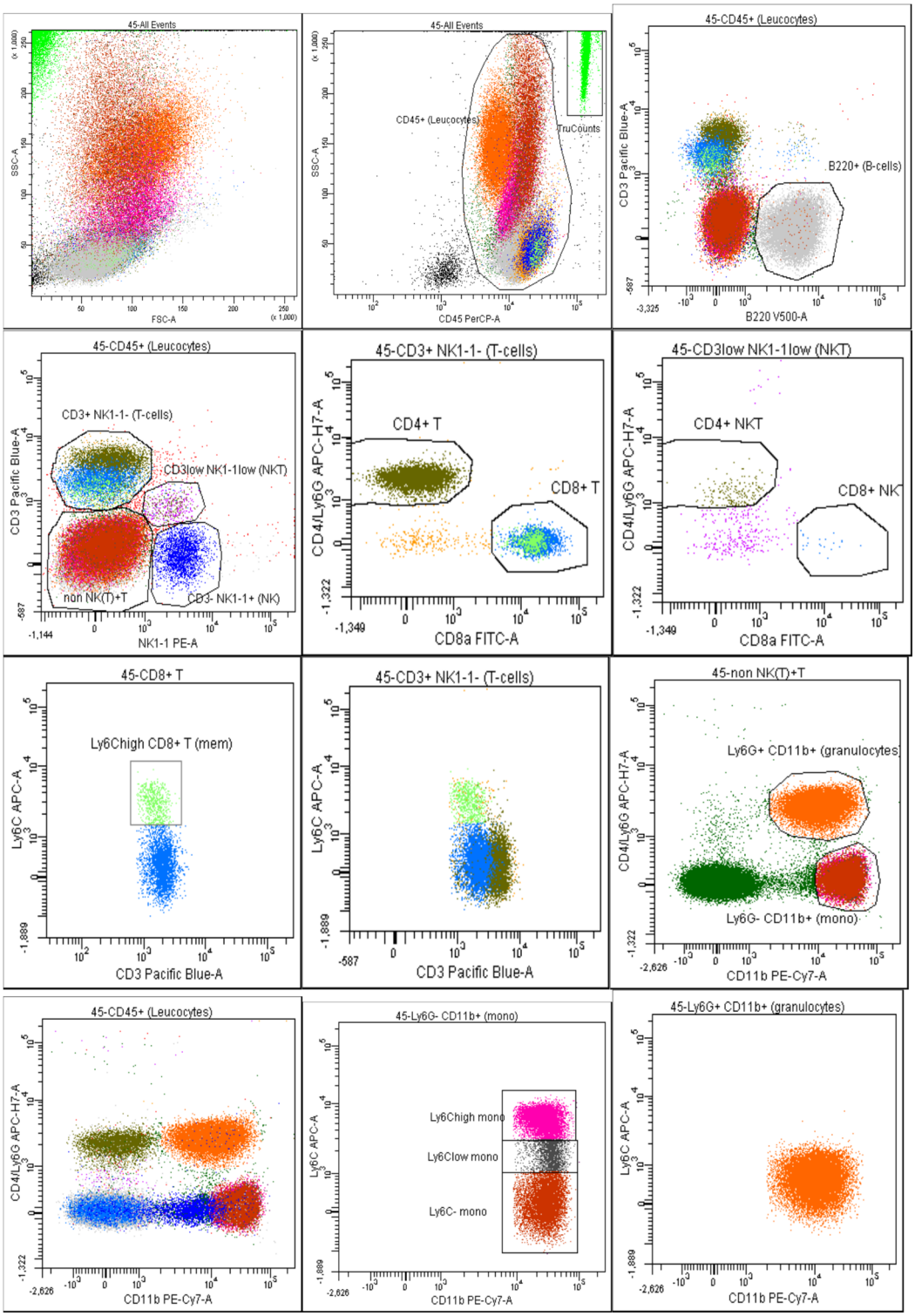

Supplementary Scheme 1. Gating strategy for Fig. 4K-N and Supp. Table 1.

Source data. Uncropped immunoblots

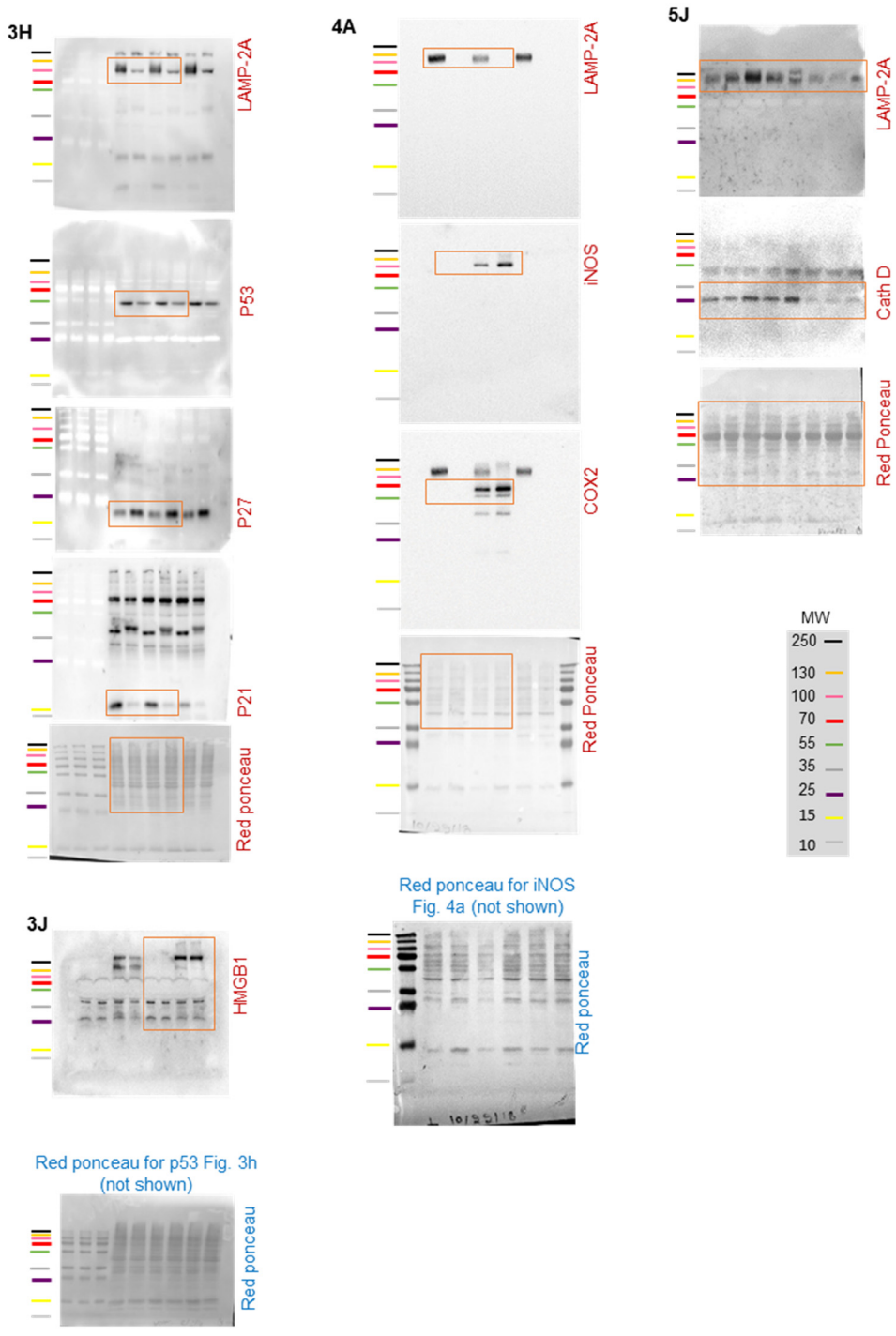

Source Data Fig. 1. Merged images of uncropped immunoblots with molecular weight markers of the immunoblot data shown in the main figures. Molecular weight markers are color coded according to the key shown.

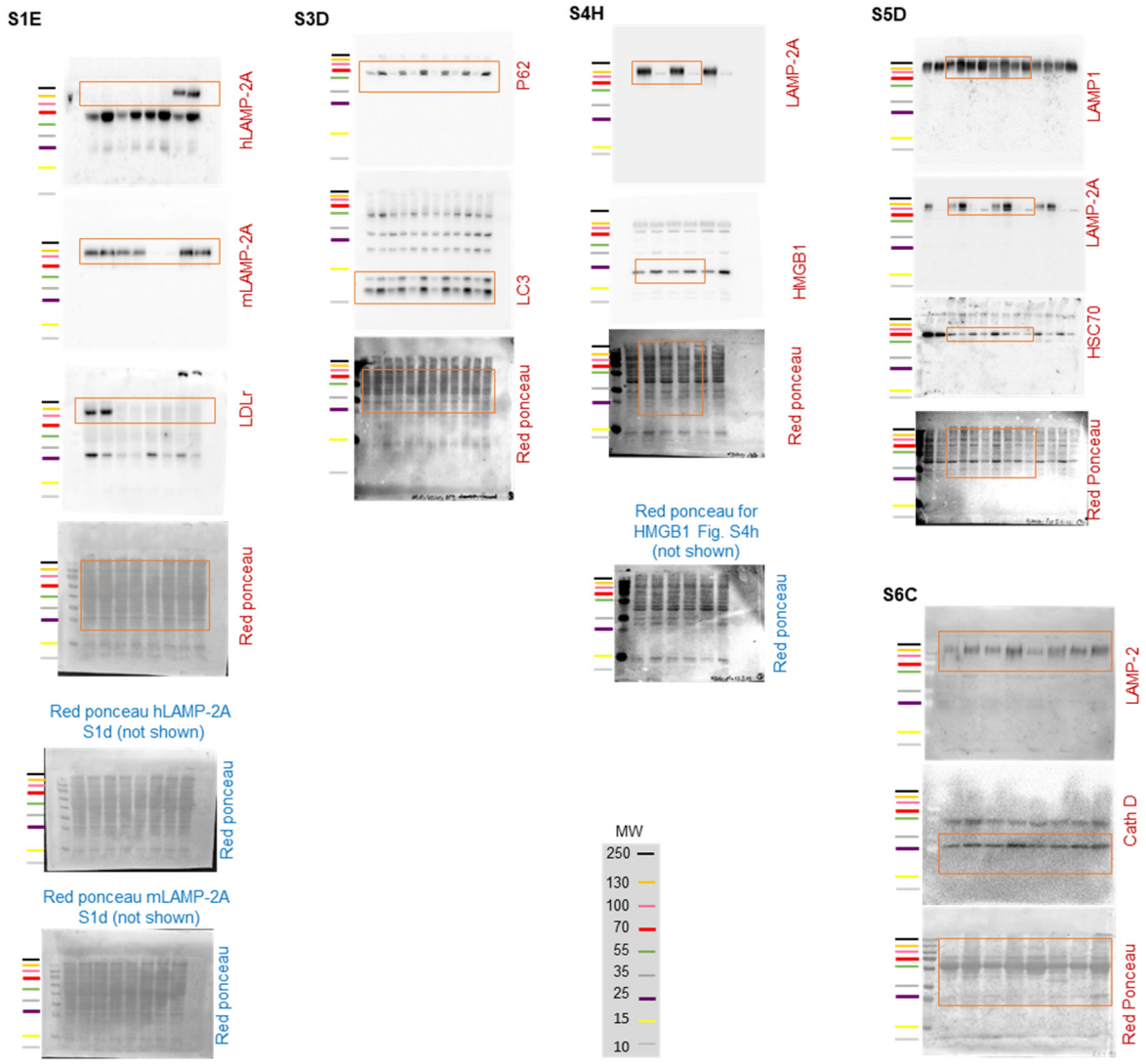

Source Data Fig. 2. Merged images of uncropped immunoblots with molecular weight markers of the immunoblot data shown in the supplementary figures. Molecular weight markers are color coded according to the key shown.

Dataset S1 (separate file). Raw data and full statistical reports (Main and supplementary figures). See attached excel file

SI References

1. S. Dong *et al.*, Monitoring spatio-temporal changes in chaperone-mediated autophagy *in vivo*. *Nat. Comm.* **15**, doi: 10.1186/s13024-13019-10354-13020 (2020).
2. J. L. Schneider, Y. Suh, A. M. Cuervo, Deficient chaperone-mediated autophagy in liver leads to metabolic dysregulation. *Cell Metab* **20**, 417-432 (2014).
3. S. Dong *et al.*, Chaperone-mediated autophagy sustains haematopoietic stem-cell function. *Nature* **591**, 117-123 (2021).
4. M. M. Bjorklund *et al.*, Induction of atherosclerosis in mice and hamsters without germline genetic engineering. *Circ Res* **114**, 1684-1689 (2014).
5. W. J. Huh *et al.*, Tamoxifen induces rapid, reversible atrophy, and metaplasia in mouse stomach. *Gastroenterology* **142**, 21-24 e27 (2012).
6. E. Araldi *et al.*, Lanosterol Modulates TLR4-Mediated Innate Immune Responses in Macrophages. *Cell Rep* **19**, 2743-2755 (2017).
7. C. A. Argmann *et al.*, Human smooth muscle cell subpopulations differentially accumulate cholesteryl ester when exposed to native and oxidized lipoproteins. *Arterioscler Thromb Vasc Biol* **24**, 1290-1296 (2004).
8. A. Canfran-Duque *et al.*, Macrophage deficiency of miR-21 promotes apoptosis, plaque necrosis, and vascular inflammation during atherogenesis. *EMBO Mol Med* **9**, 1244-1262 (2017).
9. F. O. Martinez, S. Gordon, M. Locati, A. Mantovani, Transcriptional profiling of the human monocyte-to-macrophage differentiation and polarization: new molecules and patterns of gene expression. *J Immunol* **177**, 7303-7311 (2006).
10. H. Jin *et al.*, Integrative multiomics analysis of human atherosclerosis reveals a serum response factor-driven network associated with intraplaque hemorrhage. *Clin Transl Med* **11**, e458 (2021).
11. R. Virmani, F. D. Kolodgie, A. P. Burke, A. Farb, S. M. Schwartz, Lessons from sudden coronary death: a comprehensive morphological classification scheme for atherosclerotic lesions. *Arterioscler Thromb Vasc Biol* **20**, 1262-1275 (2000).
12. R. C. Wirka *et al.*, Atheroprotective roles of smooth muscle cell phenotypic modulation and the TCF21 disease gene as revealed by single-cell analysis. *Nat Med* **25**, 1280-+ (2019).
13. W. E. Hellings *et al.*, Composition of carotid atherosclerotic plaque is associated with cardiovascular outcome: a prognostic study. *Circulation* **121**, 1941-1950 (2010).
14. J. Lonsdale *et al.*, The Genotype-Tissue Expression (GTEx) project. *Nature Genetics* **45**, 580-585 (2013).
15. T. T. S. Consortium, S. R. Quake, The Tabula Sapiens: a multiple organ single cell transcriptomic atlas of humans. *bioRxiv* 10.1101/2021.07.19.452956, 2021.2007.2019.452956 (2021).
16. S. Kaushik, A. M. Cuervo, Degradation of lipid droplet-associated proteins by chaperone-mediated autophagy facilitates lipolysis. *Nature cell biology* **17**, 759-770 (2015).

17. E. Lutgens *et al.*, Deficient CD40-TRAF6 signaling in leukocytes prevents atherosclerosis by skewing the immune response toward an antiinflammatory profile. *J Exp Med* **207**, 391-404 (2010).

18. D. Olmeda *et al.*, Whole-body imaging of lymphovascular niches identifies pre-metastatic roles of midkine. *Nature* **546**, 676-680 (2017).

19. H. Koga, M. Martinez-Vicente, F. Macian, V. V. Verkhusha, A. M. Cuervo, A photoconvertible fluorescent reporter to track chaperone-mediated autophagy. *Nat Commun* **2**, 386 (2011).

20. E. Arias *et al.*, Lysosomal mTORC2/PHLPP1/Akt Regulate Chaperone-Mediated Autophagy. *Mol Cell* **59**, 270-284 (2015).

21. B. Storrie, E. A. Madden, Isolation of subcellular organelles. *Methods Enzymol* **182**, 203-225 (1990).

22. M. Bourdenx *et al.*, Chaperone-mediated autophagy prevents collapse of the neuronal metastable proteome. *Cell* **184**, 2696-2714 e2625 (2021).

23. P. Kirchner *et al.*, Proteome-wide analysis of chaperone-mediated autophagy targeting motifs. *PLoS Biol* **17**, e3000301 (2019).

24. J. Madrigal-Matute *et al.*, HSP90 inhibition by 17-DMAG attenuates oxidative stress in experimental atherosclerosis. *Cardiovasc Res* **95**, 116-123 (2012).

25. S. Kimura, T. Noda, T. Yoshimori, Dissection of the autophagosome maturation process by a novel reporter protein, tandem fluorescent-tagged LC3. *Autophagy* **3**, 452-460 (2007).